

A small molecule that displays marked reactivity toward copper– versus zinc–amyloid- β implicated in Alzheimer's disease†

Cite this: DOI: 10.1039/c3cc48473d

Received 6th November 2013,
Accepted 20th November 2013

DOI: 10.1039/c3cc48473d

www.rsc.org/chemcomm

Alzheimer's disease (AD) is a complex, multifactorial, neurodegenerative disease that poses tremendous difficulties in pinpointing its precise etiology. A toolkit, which specifically targets and modulates suggested key players, may elucidate their roles in disease onset and progression. We report high-resolution insights on the activity of a small molecule (L2-NO) which indicates reactivity toward Cu(II)–A β over Zn(II)–A β .

Alzheimer's disease (AD) currently affects an estimated 24 million people, and starts with mild cognitive impairment, advancing to severe dementia, and ultimately death.^{1,2} Multiple pathological factors are possibly linked to AD pathogenesis.^{2,3} Amyloid- β (A β), a proteolytic product of amyloid precursor protein (APP), is found in senile plaques (SP), a hallmark of AD brains.^{2,3} Associated with SP, possibly with A β aggregated within, are high amounts of metals, e.g., Cu (ca. 0.4 mM), Zn (ca. 1 mM), and Fe (ca. 0.9 mM), when compared to healthy tissue.^{3,4}

The amyloid cascade hypothesis proposes that A β , in various forms, is responsible for neurodegeneration.^{2,3} Despite the high level of transition metals associated with A β , the precise molecular mechanism leading to A β pathogenicity with metals has not been clarified. Tools to specifically target metal–A β are necessary to interrogate the links between A β and metals and their involvement in AD. In addition, oxidative stress, another feature in AD, could be connected to A β and metals.^{2–5} Therefore, tools are needed to target A β , metals, and reactive oxygen species (ROS) to delineate the role that each plays in AD pathogenesis.^{6–9}

Previously, we reported a bifunctional molecule L2-b (Fig. 1) that targeted both A β and metals, and could modulate

Masha G. Savelieff,^a Yuzhong Liu,^a Russell R. P. Senthamarai,^{bc} Kyle J. Korshavn,^b Hyuck Jin Lee,^b Ayyalusamy Ramamoorthy^{*bc} and Mi Hee Lim^{*abd}

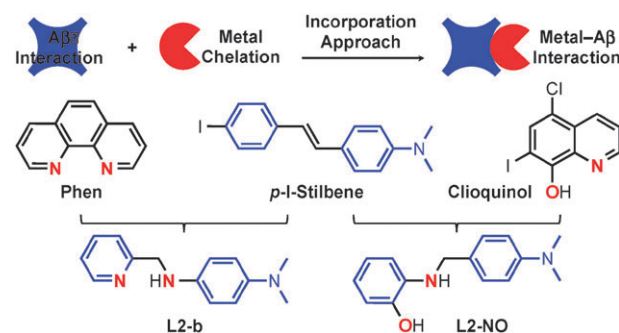


Fig. 1 Incorporation approach to design small molecules to target metal–A β species and regulate their aggregation. Phen: 1,10-phenanthroline; clioquinol = 5-chloro-7-iodoquinolin-8-ol; *p*-I-stilbene = (*E*)-4-(4-iodostyryl)-*N,N*-dimethylaniline; L2-b = *N,N'*-dimethyl-*N''*-(pyridin-2-ylmethyl)benzene-1,4-diamine; L2-NO = 2-((4-(dimethylamino)-benzyl)amino)phenol.

metal-induced A β aggregation.⁷ The design (incorporation approach)^{6–8} is based on a known A β imaging agent, a *p*-I-stilbene derivative, into which nitrogen (N) donor atoms for metal chelation are introduced. L2-b was reactive toward both Cu(II)/Zn(II)–A β (controlled their aggregation), mediated Cu–A β -triggered ROS formation, and conformed to Lipinski's rules and the calculated $-\log$ BB value for potential blood–brain barrier (BBB) permeability.⁷ To demarcate the roles of A β , metals, and oxidative stress, a tool capable of specifically interacting and reacting with redox active metal–A β species (Cu–A β) is desirable, since they may participate in Fenton-like reactions leading to toxicity.^{2–5}

Earlier, we noted a proportional relation between a ligand's metal affinity and its ability to modulate metal-induced A β aggregation. The strong ligand L2-b exhibits reactivity toward metal–A β ,⁷ whereas ligands with lower metal affinity, our diphenylpropynone derivatives were reactive with metal–A β to varying extents.¹⁰ Cu(II) is the highest in the Irving–Williams series, which ranks metals according to stability of metal–ligand complexes.¹¹ Ligands with two N donor atoms generally confer greatest stability to complexes of late, first-row transition metal ions (i.e., Ni(II), Cu(II), Zn(II)), followed by ligands with N,O and O,O donor atoms.¹¹

^a Life Sciences Institute, University of Michigan, Ann Arbor, MI 48109, USA

^b Department of Chemistry, University of Michigan, Ann Arbor, MI 48109, USA

^c Department of Biophysics, University of Michigan, Ann Arbor, MI 48109, USA.

E-mail: ramamoor@umich.edu

^d School of Nano-Bioscience and Chemical Engineering, Ulsan National Institute of Science and Technology (UNIST), Ulsan 689-798, Korea.

E-mail: mhl@unist.ac.kr

† Electronic supplementary information (ESI) available: Details of experimental procedures. See DOI: 10.1039/c3cc48473d

1 **L2-b** (N,N-donation) is expected to form more stable Cu(II) complexes than diphenylpropynone derivatives with N,O-donation (carbonyl-O). Thus, **L2-b** binds metals strongly enough to react with both Cu(II)-/Zn(II)-A β ,⁷ while diphenylpropynone derivatives
 5 interact less strongly with metal ions and their reactivity toward metal-A β is more varied.¹⁰ A ligand of intermediate strength with N,O-donation (hydroxyl-O, stronger than carbonyl-O) could target and react with Cu(II)- over Zn(II)-A β . To compare to **L2-b**, we introduced N,O donor atoms into a stilbene derivative framework.
 10 Thus, **L2-NO** (Fig. 1) was envisioned as a candidate to discern Cu(II)-A β from Zn(II)-A β , relative to **L2-b**. Design considerations of **L2-NO** are further described in the ESI†

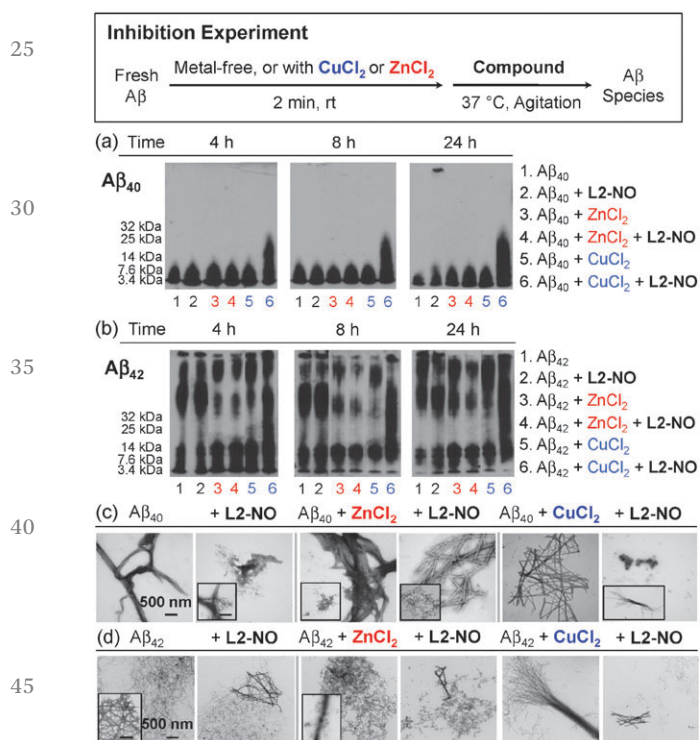
Biochemical and physical investigations were conducted to demonstrate that **L2-NO** reacts with Cu(II)-A β over Zn(II)-A β employing both A β ₄₀ and A β ₄₂. A β species from inhibition experiments (influence on A β aggregate formation) were first analysed using gel electrophoresis (Fig. 2a and b, experimental details in the ESI†). A ligand capable of modulating A β aggregation could generate A β species of various molecular weights (a broad size distribution of A β) that appears as a streak along the gel lane. Compared to compound-free samples, a streaking pattern of the

gel was exhibited only from the Cu(II)-treated A β _{40/42} samples upon incubation with **L2-NO** (Fig. 2a and b). These results suggest that **L2-NO** is able to control A β aggregation induced by Cu(II) over metal-free or Zn(II). Gel electrophoresis results were substantiated by transmission electron microscopy (TEM) (Fig. 2c and d). Aggregate morphology for metal-free and Zn(II)-treated A β ₄₀ with and without **L2-NO** was broadly similar with fibrils and some amorphous aggregates (inset) (Fig. 2c). The greatest morphological difference occurred for Cu(II), where **L2-NO**-free samples had fibrils, while **L2-NO**-treated samples comprised mainly amorphous aggregates. They also contained shorter incomplete fibrils with frayed edges (inset). TEM observations with A β ₄₂ were comparable to A β ₄₀ (Fig. 2d) with the most noticeable difference from the sample of Cu(II)-A β ₄₂ incubated with **L2-NO**.

In disaggregation experiments (**L2-NO**'s ability to disassemble preformed aggregates; Fig. S1, ESI†), A β aggregates, metal-free or with Cu(II) or Zn(II), were generated upon 24 h incubation, and then treated with **L2-NO**. In gel experiments (Fig. S1a and b, ESI†), comparison of compound-free to compound-treated lanes, for A β ₄₀ and A β ₄₂, showed distinct smearing patterns for Cu(II)-treated samples, with partial reactivity against Zn(II)-A β ₄₂ (Fig. S1, ESI†). TEM images for disaggregation samples revealed similar morphologies of A β species as inhibition experiments, where the difference between compound-free and compound-incubated samples was most pronounced in Cu(II) samples (Fig. S1c and d, ESI†). Overall, inhibition and disaggregation studies suggest that **L2-NO** is preferentially reactive toward Cu(II)-A β over metal-free A β and Zn(II)-A β . These findings for **L2-NO** contrast with **L2-b** which reacts with both Cu(II)-A β and Zn(II)-A β ,⁷ and validate our design approach for the metal preference of **L2-NO**.

The atomic-level interaction between **L2-NO** and A β ₄₀ was investigated using 2D band-selective optimized flip-angle short transient (SOFAST)-heteronuclear multiple quantum correlation (HMQC) NMR.¹² **L2-NO** was titrated (0 to 10 equiv.) into ¹⁵N-labeled A β ₄₀. Modest chemical shift perturbations (CSP) were observed for most residues, but significant changes were observed for E11, V18, F20, and M35 (Fig. 3). Changes observed for V40 are due to the intrinsic C-terminal disorder. The presence of modest CSP in most residues suggests that **L2-NO** induces a global conformational change in A β ₄₀, whilst interacting most strongly with E11, V18, F20, and M35, which is similar to **L2-b** (Fig. S2, ESI†). Importantly, our NMR data demonstrates an **L2-NO**-A β ₄₀ interaction as hypothesized in the design concept. This interaction with A β ₄₀ was confirmed by isothermal calorimetric titration (ITC) (Fig. S3, ESI†), which indicated a small, but consistent, $\Delta H = -12 (\pm 5) \text{ kJ mol}^{-1}$ upon mixing. The small, but existing, interaction of **L2-NO** with metal-free A β ₄₀ shown by NMR and ITC confirms their molecular communication. In the presence of Cu(II), the interactions of **L2-NO** with both the metal and A β result in noticeable modulation of Cu(II)-triggered aggregation.

Metal binding of **L2-NO** was studied using UV-visible spectroscopy (UV-vis).¹⁴ Cu(II) binding to **L2-NO** was confirmed by observation of the spectral changes (Fig. S4c, ESI†). Metal selectivity was performed by adding divalent metal ions to **L2-NO** (Fig. 4 and Fig. S4, ESI†). When **L2-NO** was incubated with 1 or 25 equiv. of Mg(II), Ca(II), Mn(II), Co(II), Ni(II), or Zn(II), no spectral changes were observed



Q3 Fig. 2 **L2-NO**'s influence on metal-free and metal-induced A β aggregation *in vitro*. Top: scheme for the inhibition experiment. Bottom: (a) visualization of size distribution of the resulting A β and metal-A β species by gel electrophoresis/Western blot using an anti-A β antibody (6E10). The size and shape of A β aggregates determine their permeation through the gel; thus, smearing indicates a broad size distribution of A β species, (re)directed by **L2-NO** from the principal aggregation pathway. (b) TEM images of the resultant A β and metal-A β species from 24 h incubated samples. The scale bar indicates 500 nm. Experimental conditions: [A β] = 25 μ M; [CuCl₂ or ZnCl₂] = 25 μ M; [**L2-NO**] = 50 μ M; pH 6.6 (Cu(II) samples) or 7.4 (metal-free and Zn(II) samples); 4, 8, or 24 h incubation; 37 °C; constant agitation.

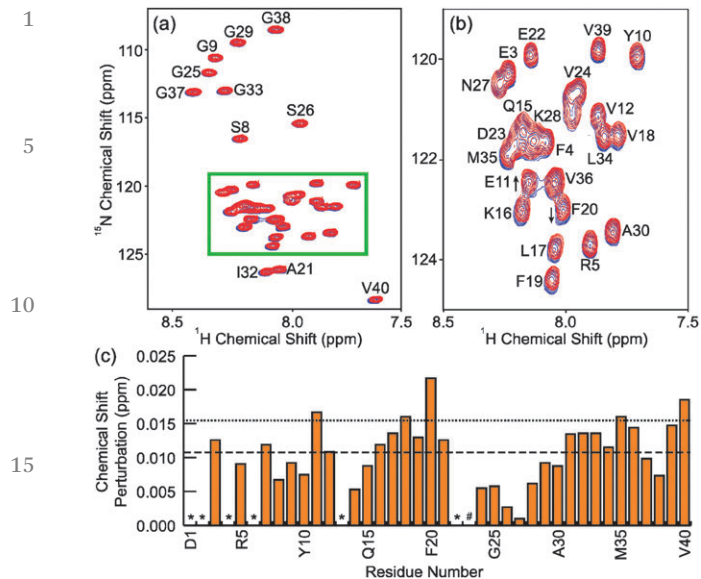


Fig. 3 SOFAST-HMQC NMR (900 MHz) spectra of uniformly-¹⁵N-labeled Aβ₄₀ with **L2-NO** (a) blue and red, 0 and 10 equiv., respectively). Resonances of Aβ₄₀ were assigned as reported previously.¹³ (b) Expanded spectra of the boxed green area of (a). (c) Normalized chemical shifts of ¹H and amide ¹⁵N atoms for all Aβ₄₀ residues (see ESI† for details). Two horizontal lines represent the average chemical shift (dashed line) plus one standard deviation (dotted line). * Residues could not be resolved for analysis (# no chemical shift was observed).

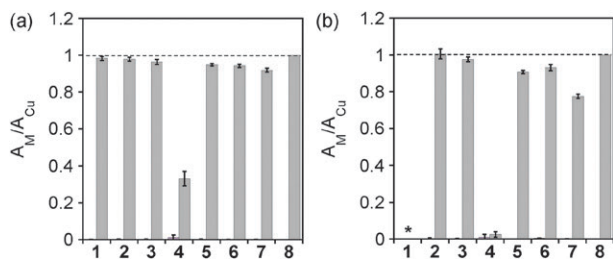


Fig. 4 Metal selectivity of **L2-NO** for Cu(II) over (a) 1 equiv. and (b) 25 equiv. of divalent metal ions, expressed as a ratio of A_M/A_{Cu} at 435 nm, prior to (purple) and following (grey) Cu(II) addition. Lanes: **1**, Mg(II); **2**, Ca(II); **3**, Mn(II); **4**, Fe(II); **5**, Co(II); **6**, Ni(II); **7**, Zn(II); **8**, Cu(II). A_M/A_{Cu} ≈ 1 after Cu(II) addition indicates selectivity for Cu(II). * Precipitation occurred.

(Fig. S5a and c, ESI†). Subsequent addition of 1 equiv. Cu(II) produced a spectrum indiscernible to **L2-NO** only treated with Cu(II), implying relative selectivity of **L2-NO** for Cu(II) (Fig. 4, Fig. S4b and d, ESI†). The spectrum of **L2-NO** with Fe(II) was unaltered; however, subsequent Cu(II) treatment of Fe(II)-added **L2-NO** did not revert the spectrum fully to Cu(II)-**L2-NO** suggesting Fe(II) interaction with **L2-NO** (Fig. 4, Fig. S4e and f, ESI†). Overall, **L2-NO** is relatively selective for Cu(II) over most divalent metal ions, with the exception of Fe(II).

The trolox equivalent antioxidant capacity (TEAC) of **L2-NO** is 2.2 (±0.2) (for **L2-b**, 2.4 (±0.2)), compared to 1.0 (±0.1) for trolox (vitamin E analogue, a known antioxidant) (Fig. S6a, ESI†).¹⁵ The antioxidant ability of **L2-NO** was pH dependent (Fig. S6a, ESI†). In addition, **L2-NO** could control Cu(II)-triggered hydroxyl radical ([•]OH) production, as confirmed by a 2-deoxyribose assay

(Fig. S6b, ESI†).¹⁶ **L2-NO** reduced [•]OH generation by ca. 50% (**L2-b**, ca. 70%) in comparison to compound-free samples. Both studies demonstrate that **L2-NO** can scavenge ROS and regulate its formation. Lastly, **L2-NO**, as for **L2-b**,⁷ was predicted to be BBB permeable by calculated values (i.e., log BB = 0.007) and experimental data (−log P_e = 4.50 (±0.06), obtained by a parallel artificial membrane permeability assay) (Table S1, ESI†).

A small molecule with structural moieties for metal chelation and Aβ interaction was designed using coordination chemistry principles¹¹ to target and react with Cu(II)-Aβ over Zn(II)-Aβ. The design concept was validated by various biochemical and physical studies, which demonstrated that **L2-NO** exhibited the modulation of Aβ aggregation triggered by Cu(II) over Zn(II). Aβ interaction with **L2-NO** was confirmed by 2D SOFAST-HMQC NMR and ITC. In addition, **L2-NO** could control oxidative stress as a potent antioxidant and regulator of ROS production. Taken together, our present studies demonstrate the feasibility of constructing a small molecule capable of specific reactivity against redox active metal-Aβ. This work will be a stepping-stone in the preparation of a toolkit of bifunctional small molecules for elucidating the role of metal-Aβ species in AD.

The authors declare no competing financial interest.

This study was supported by the Ruth K. Broad Biomedical Foundation, American Heart Association, Alfred P. Sloan Foundation, NSF (CHE-1253155), and the 2013 Research Fund (Project Number 1.130068.01) of Ulsan National Institute of Science and Technology (to M.H.L.), and NIH (GM095640 to A.R.). We thank Akiko Kochi, Younwoo Nam, & Dr Janarthanan Krishnamoorthy for experimental assistance.

Notes and references

- 1 Alzheimer's Association, *Alzheimer's Dement.*, 2012, **8**, 131–168.
- 2 R. Jakob-Roetne and H. Jacobsen, *Angew. Chem., Int. Ed.*, 2009, **48**, 3030–3059.
- 3 M. G. Savelieff, S. Lee, Y. Liu and M. H. Lim, *ACS Chem. Biol.*, 2013, **8**, 856–865.
- 4 A. S. Pithadia and M. H. Lim, *Curr. Opin. Chem. Biol.*, 2012, **16**, 67–73.
- 5 A. Rauk, *Chem. Soc. Rev.*, 2009, **38**, 2698–2715.
- 6 J.-S. Choi, J. Braymer, R. P. Nanga, A. Ramamoorthy and M. H. Lim, *Proc. Natl. Acad. Sci. U. S. A.*, 2010, **107**, 21990–21995.
- 7 C. Rodríguez-Rodríguez, N. Sánchez de Groot, A. Rimola, Á. Álvarez-Larena, V. Lloveras, J. Vidal-Gancedo, S. Ventura, J. Vendrell, M. Sodupe and P. González-Duarte, *J. Am. Chem. Soc.*, 2009, **131**, 1436–1451.
- 8 C. Rodríguez-Rodríguez, M. Telpoukhovskaia and C. Orvig, *Coord. Chem. Rev.*, 2012, **256**, 2308–2332.
- 9 A. K. Sharma, S. T. Pavlova, J. Kim, D. Finkelstein, N. Hawco, N. P. Rath, J. Kim and L. M. Mirica, *J. Am. Chem. Soc.*, 2012, **134**, 6625–6636.
- 10 (a) A. S. Pithadia, A. Kochi, M. T. Soper, M. W. Beck, S. Lee, A. S. DeToma, B. T. Ruotolo and M. H. Lim, *Inorg. Chem.*, 2013, **51**, 12959–12967; (b) Y. Liu, A. Kochi, A. S. Pithadia, S. Lee, Y. Nam, M. W. Beck, X. He, D. Lee and M. H. Lim, *Inorg. Chem.*, 2013, **52**, 8121–8130.
- 11 H. Irving and R. J. P. Williams, *J. Chem. Soc.*, 1953, 3192–3210.
- 12 S.-J. Hyung, A. S. DeToma, J. R. Brender, S. Lee, S. Vivekanandan, A. Kochi, J.-S. Choi, A. Ramamoorthy, B. T. Ruotolo and M. H. Lim, *Proc. Natl. Acad. Sci. U. S. A.*, 2013, **110**, 3743–3748.
- 13 S. Vivekanandan, J. R. Brender, S. Y. Lee and A. Ramamoorthy, *Biochem. Biophys. Res. Commun.*, 2011, **411**, 312–316.
- 14 **L2-NO** is susceptible to oxidation by redox-active metals in protic solvents (Fig. S4a and b, ESI†); thus, metal binding was studied in CH₃CN.
- 15 R. Re, N. Pellegrini, A. Proteggente, A. Pannala, M. Yang and C. Rice-Evans, *Free Radical Biol. Med.*, 1999, **26**, 1231–1237.
- 16 L. K. Charkoudian, D. M. Pham and K. J. Franz, *J. Am. Chem. Soc.*, 2006, **128**, 12424–12425.